MATERIALS COMMUNICATIONS

The purpose of this Materials Communications section is to provide accelerated publication of important new results in the fields regularly covered by Journal of Materials Research. Materials Communications cannot exceed four printed pages in length, including space allowed for title, figures, tables, references, and an abstract limited to about 100 words.

Temperature dependence of the indentation size effect

Oliver Franke, Jonathan C. Trenkle, and Christopher A. Schuh[a)]
Department of Materials Science and Engineering, Massachusetts Institute of Technology, Cambridge, Massachusetts 02139

(Received 8 January 2010; accepted 30 March 2010)

The influence of temperature on the indentation size effect is explored experimentally. Copper is indented on a custom-built high-temperature nanoindenter at temperatures between ambient and 200 °C, in an inert atmosphere that precludes oxidation. Over this range of temperatures, the size effect is reduced considerably, suggesting that thermal activation plays a major role in determining the length scale for plasticity.

The indentation size effect (ISE) is a widely discussed phenomenon where the measured hardness of a crystalline material increases as the indentation depth is reduced.[1–8] The ISE becomes more pronounced at very low displacements into the surface, such as are usually encountered in nanoindentation. The physical origins of the ISE are generally believed to lie in the strain gradients produced beneath the indentation and the associated geometrically necessary dislocations (GNDs). While strain gradient plasticity was extensively developed in the works of Fleck and Hutchinson,[9–13] the ISE was first addressed in this context by Nix and Gao.[7] Their work provided the basic explanation for the ISE resulting from the surplus of dislocations needed to accommodate the impression geometry at low displacements. Support for this notion is provided by experiments showing that there is no ISE for materials with pre-existing high dislocation densities (such as ultrafine-grained materials produced by severe plastic deformation[3]) or for amorphous materials (e.g., the fused quartz samples used to calibrate nanoindenters[14,15]). More recent studies on the ISE by Durst and co-workers[1–4,16] have emphasized how the size of the plastic zone exerts a significant influence on the ISE.

Although there seems to be some consensus that the distribution of dislocations is central to the observation of the ISE, studies that specifically vary the dislocation properties (i.e., mobility, stacking fault width, etc.) and examine the result on the ISE are very few. For example, we are not aware of any studies on ISE at nonambient temperatures, although dislocation source activity, cross-slip, and junction stability are all significantly temperature dependent; small changes in temperature could lead to significant changes in the details of the ISE, and thereby offer more insight into its physical origins. In fact, the onset and early stages of plasticity in nanoindentation of single crystals are already known to be significantly temperature dependent, although how such effects translate to the ISE remains unexplored.[17,18] In this manuscript we provide some preliminary observations along these lines, by studying the ISE in Cu at both ambient and elevated temperatures.

A copper sample of technical purity (99.95%, Online Metals, Seattle, WA) was mechanically polished to mirror smoothness. The grain size was about 2–3 mm, permitting all of the indentations reported below to be carried out essentially within a single crystal (albeit of unknown orientation). For shallow nanoindentations, oxide growth is a significant concern, especially at elevated temperatures; accordingly, our experiments were conducted on a custom apparatus[19,20] based on a Hysitron (Minneapolis, MN) Ubi1 indenter, housed in a vacuum/atmosphere chamber. Prior to testing, the chamber was cyclically purged by mechanical vacuum and refilled with high purity Ar. Testing was conducted in a partial vacuum of 10^{-2} Torr, with the residual gas in the chamber being Ar.

The indentation experiments were carried out using a triangular load function with a hold segment at the 20% unload condition to measure the drift rate. The maximum drift rate increased with temperature from around 0.1 nm/s at room temperature to about 7 nm/s at 200 °C. A relatively high loading rate of 5 mN/s was chosen to guarantee that the accumulated drift displacement over the course of the test was usually less than 4 nm, and always less than 11 nm (which translates into a hardness error of less than 5%). For each temperature (23, 150, and 200 °C) and maximum load (1, 2, 3, 4, 5, and 6 mN, and also 7 mN at 23 and 200 °C), a minimum of 25 indentations were analyzed; we report the mean values here with error bars reflective of the standard deviations. The change in peak

[a)]Address all correspondence to this author.
e-mail: schuh@mit.edu
This author was an editor of this journal during the review and decision stage. For the *JMR* policy on review and publication of manuscripts authored by editors, please refer to http://www.mrs.org/jmr_policy
DOI: 10.1557/JMR.2010.0159

load causes a change in the strain rate, although only over a small range (less than an order of magnitude) that should have no influence on the results, since copper has a negligible strain-rate dependence over the tested range.

The load–displacement (P–h) curves we recorded were very reproducible even for the higher temperatures, as illustrated by the series of typical curves presented in Fig. 1. The hardness was calculated for all seven tested loads using the calibrated tip area function (which is, to an excellent approximation, constant with temperature[19]) and the Oliver–Pharr method.[14] Figure 2 summarizes the hardness values, H, obtained at all three test temperatures, as a function of the contact depth, h_c. Here, we observe that for relatively deeper indentations, the hardness declines only slightly with increasing test temperature (by ~12% from 23 to 200 °C). As the indentation depth is reduced to the nanoscale, we observe the increase in H that is characteristic of the ISE. However, it can clearly be seen that the ISE is less pronounced at the higher temperatures, even though the maximum test temperature of 200 °C is still relatively low (homologous temperature of 0.35). For a low applied load of 1 mN, the hardness drops by almost 25% from 23 to 200 °C.

We provide further analysis of the ISE following the works of Nix and Gao[7] as well as Durst et al.[2–4] Within their framework, the displacement dependence of the hardness is given by

$$H = H_0\left(1 + \frac{h^*}{h_c}\right)^{1/2} , \qquad (1)$$

where H_0 is the so-called "infinite hardness," corresponding to the hardness at the infinite indentation depth, and h^* is the material length scale parameter. Figure 3 shows our data from Fig. 2, replotted in the form suggested by Eq. (1), along with the linear least squares fits using H_0 and h^* as adjustable parameters; the best-fit values of these parameters are given in Table I.

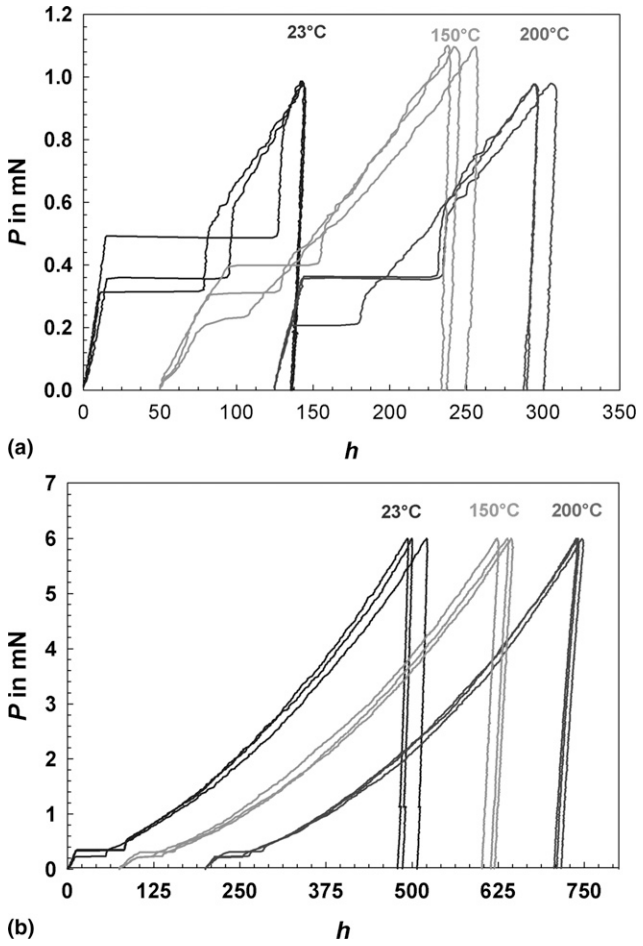

FIG. 1. Load–displacement curves for two different loads (a) 1 mN and (b) 6 mN at the tested temperatures. Note that three randomly selected load–displacement curves for each load and temperature are shown. The sets of curves are offset along the x axis for clarity of observation.

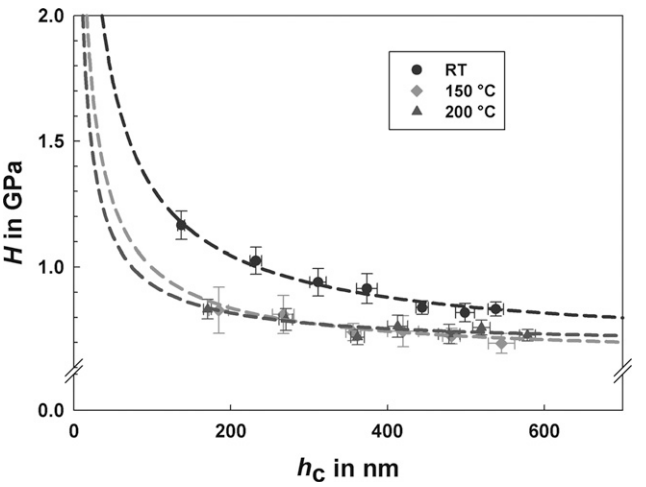

FIG. 2. Hardness as a function of the displacement for all three temperatures; the dashed lines show the best fits of Eq. (1).

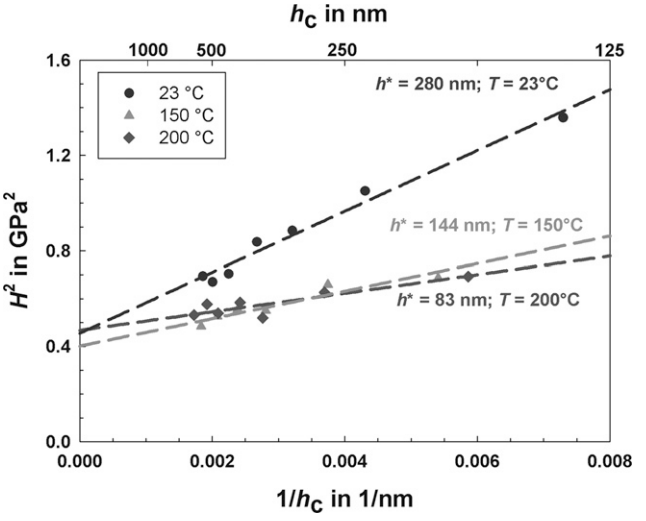

FIG. 3. Nix–Gao plot of the indentation size effect in copper at three temperatures. The lines show the best fits of Eq. (1).

TABLE I. Extracted fitting parameters based on Eqs. (1) and (4), including the infinite hardness H_0 and the plasticity length scale h^*, as well as the apparent storage volume of GNDs and the coefficient of determination (R^2) for each fit.

T in °C	H_0 in MPa	h^* in nm	R^2	f
23	675	280	0.98	1.8
150	638	144	0.89	2.2
200	687	83	0.78	2.6

H_0, which is determined from the intercept in Fig. 3, is found to be roughly constant over the studied temperature range (Fig. 3), with the spread of best fit H_0 values spanning only ~50 MPa. This difference is small, being of a similar magnitude to the 5% error range associated with our raw hardness measurements in the first place. This result is reasonable in light of the small temperature dependence of the yield strength of copper, which reduces by only ~28 MPa over this range of temperatures.[21] Prior hot microhardness measurements also reflect only mild decreases in hardness over this range (~120 MPa in Ref. 22, 85 ± 9 MPa in Ref. 23, and 74–131 MPa in the compiled data of Ref. 24) and no significant influence of the dwell time for temperatures up to 220 °C.[23]

More significant than H_0 is h^*, which is referred to as the material-dependent plasticity length scale,[7] and which is proportional to the slope in Fig. 3. We find that as T rises, h^* declines considerably in copper, from ~280 nm at room temperature to only ~80 nm at 200 °C. The former value is in line with expectations from prior studies on Cu (which give h^* ~200–700 nm at room temperature[2,3,16]). However, the strong temperature dependence of h^* is, to our knowledge, reported here for the first time. Fleck and Hutchinson[10–12] correlated the internal material length scale to the spacing between obstacles, which, in the case of a pure metal, are other dislocations and their associated junctions and locks; the plasticity length scale h^* is interpreted as the mean free path of a dislocation.[7,10–12] In this light, our results suggest that dislocation-based obstacles are more prevalent (more finely spaced) at mildly elevated temperatures.

We can further explore the physical origins of the temperature dependence of h^* by considering Nix and Gao's equivalent form of Eq. (1), written in terms of dislocation densities:

$$H = MC\alpha Gb(\rho_{SSD} + \rho_{GND})^{1/2} \quad . \tag{2}$$

Here, the Taylor factor $M = 3$, constraint factor $C \approx 3$ for fully plastic indentation, $\alpha = 0.5$, G is the shear modulus (taken to be 42, 40, and 39.2 GPa at 23, 150, and 200 °C, respectively[21]), and the Burgers vector magnitude b = 0.25 nm.[21] The symbol ρ represents the dislocation density, and the subscripts SSD and GND denote the subpopulations of statistically stored and geometrically necessary dislocations, respectively. The statistically stored dislocations comprise those contained in the material before testing as well as those required to attain the representative strain of the specific indenter geometry.[25] The GNDs are the dislocations required to form the impression in the surface and their density derives directly from the indentation geometry as[1–3,7]

$$\rho_{GND} = \frac{3}{2}\frac{1}{f^3}\frac{\tan\theta}{bh} \quad , \tag{3}$$

with θ the angle between indenter and surface, which is 19.7° for a Berkovich geometry as used here. The parameter f was assigned a value of unity by Nix and Gao,[7] but has more recently been generalized by Durst et al.[2,3] to account for variations in plastic zone size with intrinsic materials properties; f denotes the size of the storage volume of the GNDs relative to the characteristic volume obtained by cubing the contact radius, and may be thought of as the storage volume for GNDs.

Combining Eqs. (2) and (3) and rearranging gives

$$H = \rho_{SSD}^{1/2} MC\alpha Gb\left(1 + \frac{3}{2}\frac{1}{f^3}\frac{\tan\theta}{bh}\frac{1}{\rho_{SSD}}\right)^{1/2} \quad , \tag{4}$$

which, by comparison with Eq. (1), suggests that

$$H_0 = MC\alpha Gb\rho_{SSD}^{1/2} \quad , \tag{5}$$

and

$$h^* = \frac{3}{2}\frac{1}{f^3}\frac{\tan\theta}{b}\frac{1}{\rho_{SSD}} \quad . \tag{6}$$

In this expression, the indenter angle and Burgers vector are constants for the present experiments, suggesting that either f or ρ_{SSD}, or both, must increase with temperature in order to account for the decrease in the plasticity length scale that we observe in our experiments. Both of these possibilities have some precedent in prior discussions in the literature on nanoindentation; we consider the possible effects of f and ρ_{SSD} separately in what follows.

Our fitted values of H_0 and h^* can be translated to provide values for the parameter f, as shown in Table I. Here, we observe a rise from $f = 1.8$ to 2.6 as temperature increases from 23 to 200 °C. The room temperature value is in line with a prior value for copper prepared by mechanical polishing,[16] and somewhat lower than can be achieved in an electropolished sample.[2,16] In their work on solid solutions at room temperature, Durst and coworkers[4] observed changes in h^* with alloy chemistry, and attributed these to the effect of solutes on the GND storage volume f. Following this line of reasoning, the present results may speak to the effect of temperature as increasing the characteristic volume into which GNDs are injected during nanoindentation. This seems reasonable from the point of view that temperature decreases lattice friction and increases the mobility of dislocations, and is also consistent with the increased characteristic

length scales for dislocation cell formation at higher temperatures as reported by Staker et al.[26] at 10% strain.

The second possible explanation for a decrease in h^* is related to the statistically stored dislocation content; i.e., higher temperatures may promote an increase in ρ_{SSD}. This argument is in line with prior speculations of Lund et al.,[17] who observed that as the temperature of Pt singles crystals increased, the pop-in behavior associated with dislocation activity increased considerably during very fine-scale nanoindentation measurements. The authors reasoned that mild temperature increases would promote more stochastic events in the evolution of the plastic zone (e.g., more dislocation source activations, more cross-slip, more entanglements, a greater degree of parallel slip[27,28]) through thermal activation. Even for the same impression geometry, this scenario would involve more dislocation multiplication and would lead to a higher density of statistically stored dislocations at elevated temperatures.

Both of the above effects are reasonable and it is important to recognize that they are not mutually exclusive; it is entirely plausible that temperature could increase the storage volume for GNDs (without increasing their net density) and at the same time increase the density of SSDs. In fact, since an increase in ρ_{SSD} would nominally cause an increase in H_0 with temperature [see Eq. (5)], it seems that some other effect would be required to recover the expected lowering of infinite hardness with temperature. We leave for future work the task of examining the dislocation structures beneath indentations made at various temperatures to explore these issues.

There is another possible effect of temperature that is not captured by the above arguments based solely on h^*. The Nix–Gao model assumes a parabolic hardening law with dislocation density, whereas temperature is known to affect the hardening exponent n in copper. Specifically, increasing the temperature is expected to decrease n significantly, as shown for Cu between 20 ($n = 0.48$) and 425 °C ($n = 0.41$) in Ref. 29. In terms of the above model, this may be incorporated as a change in the exponent on Eqs. (1) and (2), which would imply that the scaling of hardness simply with $(1 + 1/h)^{1/2}$ would not be attained at all temperatures (or in all materials). In this light, it is interesting to note that our experimental data fit the expected scaling of Eq. (1) with a high coefficient of determination ($R^2 = 0.98$) at room temperature, where the hardening exponent for copper is close to 0.5 in uniaxial compression,[29] but exhibit a significantly poorer fit as the temperature rises and the hardening exponent drops (see Table I). It is also interesting to note that a decrease in the work-hardening behavior with increasing temperature would resemble a transition toward elastic-ideally plastic behavior, and in this case no ISE is expected. In such cases fitting with Eq. (1) would give the internal plasticity length scale as zero ($h^* = 0$), as found in ultrafine-grained Cu produced by severe plastic deformation[3] and predicted by Shu and Fleck[30]; in this case the pre-existing dislocation content is so high as to preclude further work hardening. The apparent decrease we see in h^* with temperature here, and the corresponding decrease in the quality of fitting the data with Eq. (1), may thus anticipate a more general ISE model that permits some variability in the work-hardening exponent.

Before concluding, we observe that any proposed explanation for the temperature dependence of the ISE must be rooted in the dynamics of conservative dislocation activity. Diffusional mechanisms can be ruled out for the short duration indentation experiments conducted here, which lasted less than 15 s. Over this time the diffusion distance is only 10^{-17} m (volume diffusion at 200 °C) or 10^{-13} m (dislocation core diffusion at 200 °C with a diffusive dislocation core radius of 0.6 nm[21]); either value is too small to be significant, even for the very small scales involved in a nanoindentation.

In conclusion, we have found that the ISE decreases markedly with increasing temperature. Within the prevailing theoretical framework, this is apparently due to a decrease in the intrinsic plasticity length scale, which in turn may be due to either an increase in the characteristic volume into which geometrically necessary dislocations are deposited during indentation or to an increase in the density of statistically stored dislocations beneath the indentation, or both. However, we note that the Nix–Gao model for the ISE does not explicitly account for changes in (e.g., work-hardening exponent with temperature), so other physical explanations are possible.

ACKNOWLEDGMENTS

Financial support through the Institute for Soldier Nanotechnologies at MIT (U.S. Army Research Office) is gratefully acknowledged. The authors would like to thank Timothy Rupert (MIT) for helpful discussions.

REFERENCES

1. B. Backes, K. Durst, and M. Goken: Determination of plastic properties of polycrystalline metallic materials by nano-indentation: Experiments and finite element simulations. *Philos. Mag*. **86,** 5541 (2006).
2. K. Durst, B. Backes, O. Franke, and M. Goken: Indentation size effect in metallic materials: Modeling strength from pop-in to macroscopic hardness using geometrically necessary dislocations. *Acta Mater*. **54,** 2547 (2006).
3. K. Durst, B. Backes, and M. Goken: Indentation size effect in metallic materials: Correcting for the size of the plastic zone. *Scr. Mater*. **52,** 1093 (2005).
4. K. Durst, O. Franke, A. Bohner, and M. Goken: Indentation size effect in Ni–Fe solid solutions. *Acta Mater*. **55,** 6825 (2007).
5. A.A. Elmustafa, J.A. Eastman, M.N. Rittner, J.R. Weertman, and D.S. Stone: Indentation size effect: Large grained aluminum

versus nanocrystalline aluminum-zirconium alloys. *Scr. Mater.* **43,** 951 (2000).
6. A.A. Elmustafa and D.S. Stone: Indentation size effect in polycrystalline F.C.C. metals. *Acta Mater.* **50,** 3641 (2002).
7. W.D. Nix and H. Gao: Indentation size effects in crystalline materials: A law for strain gradient plasticity. *J. Mech. Phys. Solids* **46,** 411 (1998).
8. M. Rester, C. Motz, and R. Pippan: Indentation across size scales—A survey of indentation-induced plastic zones in copper {1 1 1} single crystals. *Scr. Mater.* **59,** 742 (2008).
9. Y. Huang, H. Gao, W.D. Nix, and J.W. Hutchinson: Mechanism-based strain gradient plasticity—II. Analysis. *J. Mech. Phys. Solids* **48,** 99 (2000).
10. N.A. Fleck and J.W. Hutchinson: A reformulation of strain gradient plasticity. *J. Mech. Phys. Solids* **49,** 2245 (2001).
11. N.A. Fleck and J.W. Hutchison: Strain gradient plasticity. *Adv. Appl. Mech.* **33,** 295 (1997).
12. N.A. Fleck, G.M. Muller, M.F. Ashby, and J.W. Hutchinson: Strain gradient plasticity: Theory and experiment. *Acta Metall. Mater.* **42,** 475 (1994).
13. H. Gao, Y. Huang, W.D. Nix, and J.W. Hutchinson: Mechanism-based strain gradient plasticity—I. Theory. *J. Mech. Phys. Solids* **47,** 1239 (1999).
14. W.C. Oliver and G.M. Pharr: An improved technique for determining hardness and elastic modulus using load and displacement sensing indentation experiments. *J. Mater. Res.* **7,** 1564 (1992).
15. M.F. Doerner and W.D. Nix: A method for interpreting the data from depth-sensing indentation instruments. *J. Mater. Res.* **1,** 601 (1986).
16. B. Backes, Y.Y. Huang, M. Göken, and K. Durst: The correlation between the internal material length scale and the microstructure in nanoindentation experiments and simulations using the conventional mechanism-based strain gradient plasticity theory. *J. Mater. Res.* **24,** 1197 (2009).
17. A.C. Lund, A.M. Hodge, and C.A. Schuh: Incipient plasticity during nanoindentation at elevated temperatures. *Appl. Phys. Lett.* **85,** 1362 (2004).
18. J.K. Mason, A.C. Lund, and C.A. Schuh: Determining the activation energy and volume for the onset of plasticity during nanoindentation. *Phys. Rev. B* **73,** 054102 (2006).
19. C.A. Schuh, C.E. Packard, and A.C. Lund: Nanoindentation and contact-mode imaging at high temperatures. *J. Mater. Res.* **21,** 725 (2006).
20. C.E. Packard: Nanomechanical studies of metallic glasses at ambient and elevated temperatures. Ph.D. Thesis, Massachusetts Institute of Technology, Cambridge, MA, 2008.
21. H.J. Frost and M.F. Ashby: *Deformation Mechanism Maps: The Plasticity and Creep of Metals and Ceramics*, 1st ed. (Pergamon Press, Oxford, UK, 1982).
22. P. Ludwik: About the change in internal friction with temperature. *Z. Phys. Chem.* **91,** 232 (1916).
23. J. Engl and G. Heidtkamp: The temperature dependence of the cone indentation hardness in metals. *Z. Phys.* **95,** 30 (1935).
24. J.H. Westbrook: Temperature dependence of the hardness of pure metals. *Trans. Am. Soc. Met.* **45,** 221 (1953).
25. A.G. Atkins and D. Tabor: Plastic indentation in metals with cones. *J. Mech. Phys. Solids* **13,** 149 (1965).
26. M.R. Staker and D.L. Holt: The dislocation cell size and dislocation density in copper deformed at temperatures between 25 and 700 °C. *Acta Metall.* **20,** 569 (1972).
27. K.A. Nibur, F. Akasheh, and D.F. Bahr: Analysis of dislocation mechanisms around indentations through slip step observations. *J. Mater. Sci.* **42,** 889 (2007).
28. K.A. Nibur and D.F. Bahr: Identifying slip systems around indentations in FCC metals. *Scr. Mater.* **49,** 1055 (2003).
29. N. Christodoulou and J.J. Jonas: Work hardening and rate sensitivity material coefficients for OFHC Cu and 99.99% A1. *Acta Metall.* **32,** 1655 (1984).
30. J.Y. Shu and N.A. Fleck: The prediction of a size effect in microindentation. *Int. J. Solids Struct.* **35,** 1363 (1998).